FIG. 2. Reduced repetition rate data as a function of temperature.

smooth curves that were drawn by eye through the data points. These smooth curves were used for the data analysis to be discussed in Sec. III. The dashed lines are straight lines representing the transit times in phase II. There are several interesting features of the transit-time data that may be noted. The most striking feature is the large increase in the shear-mode transition time in phase II, which corresponds to a decrease in the velocity. The shear velocity is a decreasing function of pressure in phase II. The changes in the longitudinal mode across the phase boundaries are much smaller than for the shear mode, and the longitudinal-mode velocity increases normally with increasing pressure in all three phases. These features are qualitatively the same as those noted in previous work.[7-9] One feature not previously reported is the large amount of curvature in the transit-time data in phase III. The work of Refs. 7 and 9 indicate nearly linear behavior of the transit times as a function of pressure in this phase. Special care was taken to establish that this curvature is real. Stable transit-time values were obtained within ~15 min after a change of pressure, and these stable values were held for times of up to 30 min for some of the points in the curved region.

The temperature data are shown in Fig. 2. Since all the temperature data were obtained by the pulse superposition technique, we have represented the data by the reduced repetition rate ratio $f(T)/f(23\,°C)$. Here f is the inverse of the transit time, $f = t^{-1}$. The relatively large amount of scatter is due to less than ideal ultrasonic bonding between the transducer and sample. These data indicate normal decreases of the acoustic velocities with increasing temperature, and are qualitatively in agreement with what one would expect based on high-temperature measurements of the single-crystal elastic constants of bismuth.[12]

III. DATA ANALYSIS

In order to determine the ultrasonic velocities as a

function of pressure and temperature from the transit-time data represented in Figs. 1 and 2, it is necessary to know the changes in the acoustic path length as the pressure or temperature is varied. The temperature correction is small because of the relatively low thermal expansion of bismuth. We used the value[13] $\alpha = 4.2 \times 10^{-5}/$ °C for the volume thermal expansion coefficient, and we assumed α to be constant over our temperature range.

The determination of the path length changes as a function of pressure requires somewhat more care because of the relatively large compressibility of bismuth and the discontinuous volume changes at the I-II and II-III phase boundaries. A number of measurements have been made of the compression of bismuth at high pressure,[1, 2, 9, 14] and these experiments have not given consistent results, especially with regard to the discontinuities at the phase boundaries. For the I-II transition, values of $\Delta V/V_0$ ranging from 3.5 to 5.8% have been given, and for the II-III transition the range is 2.7 to 3.6%. We have used the compression data of Giardini and Samara[14] for reducing our data. These authors measured the compression with a sensitive and accurate inductive coil technique, whereas the other compression measurements were made by the piston-cylinder displacement technique. Dr. Samara has kindly made his original compression data available to us.

The pressure and temperature dependences of the acoustic velocities were determined as described above from the smooth curves of Figs. 1 and 2. The high-pressure results are shown in Fig. 3 and the temperature results are tabulated in Table I. For numerical reference, the pressure data are partially tabulated in Table II. From the acoustic data, it is possible to deduce various elastic properties of bismuth as a function of pressure and temperature. In Fig. 4 we have plotted the longitudinal, shear, and bulk moduli (L, μ, and B, respectively) and Lamé's λ, as a function of pressure. These results are also partially tabulated in Table II,
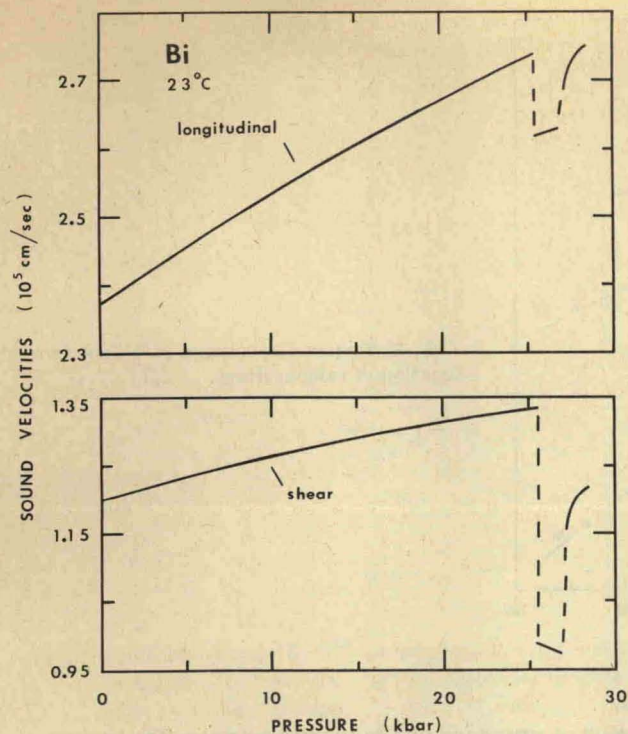
FIG. 3. Longitudinal and shear velocities as a function of pressure.

along with the Young's modulus Y and Poisson's ratio σ. The temperature dependences of the various elastic moduli are also tabulated in Table I. All values quoted for the moduli are adiabatic values. The number of significant digits retained in Tables I and II are not meant to reflect either the accuracy or the precision of the results. The over-all accuracy of the results is about 1% for the velocities and 2% for the moduli.

In Table III we have listed the temperature derivatives of the velocities and other elastic parameters at 23 and 160 °C. The Lamé λ was nearly constant with temperature and the value listed in Table III was approximated from a straight line through the whole temperature range. Pressure derivatives taken from Figs. 3 and 4 for phases I and II are listed in Table IV. The entries in Tables III and IV are considered accurate to about 7%.
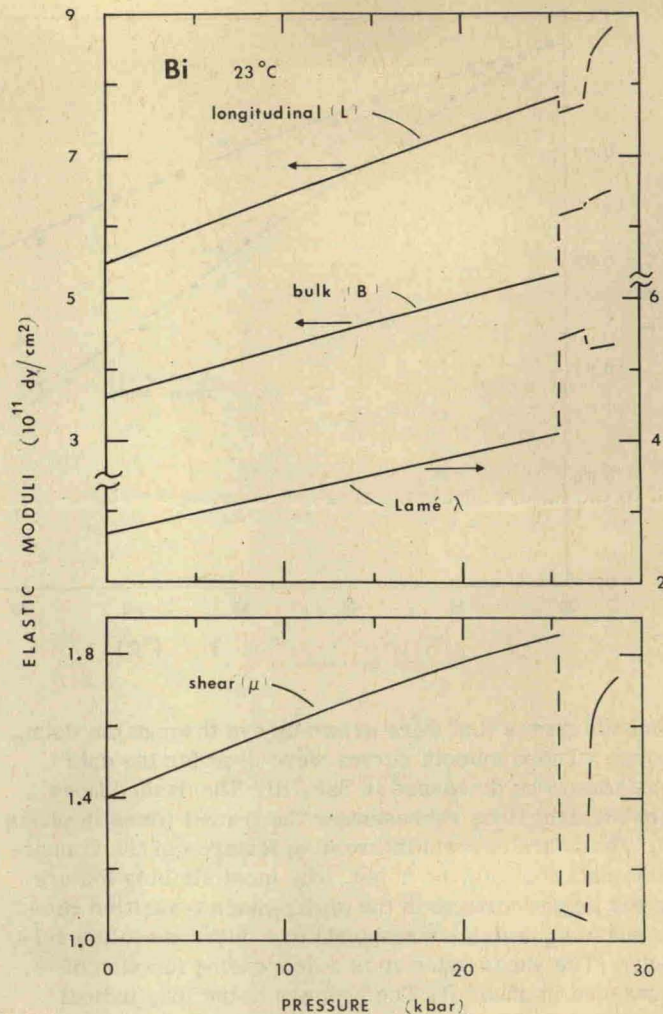

FIG. 4. Pressure dependences of various elastic moduli.

IV. DISCUSSION AND CONCLUSION

The present data have been used by Johnson et al.[6] to help define the equation of state of Bi II. These authors used a constant value of $B=615$ kbar for phase II, and, in the absence of specific heat data, they assumed that C_V has the Dulong-Petite value of $3R$. Reference 6 may be consulted for further details of the equation-of-state determination and for details of stress-wave calculations

TABLE I. Temperature dependences of various elastic properties of polycrystalline bismuth as calculated from smooth curves of Fig. 2. The quantities tabulated are longitudinal velocity v_l; shear velocity v_t; longitudinal modulus L; shear modulus μ; Lamé λ; Young's modulus Y; and Poisson's ration σ.

T (°C)	v_l (10^5 cm/sec)	v_t (10^5 cm/sec)	L (10^{10} dyn/cm^2)	μ (10^{10} dyn/cm^2)	λ (10^{10} dyn/cm^2)	Y (10^{10} dyn/cm^2)	B (10^{10} dyn/cm^2)	σ
20	2.376	1.201	54.93	14.04	26.85	37.30	36.21	0.3283
40	2.369	1.194	54.57	13.86	26.85	36.86	36.09	0.3297
60	2.362	1.186	54.21	13.67	26.85	36.40	35.96	0.3314
80	2.354	1.178	53.78	13.48	26.82	35.93	35.81	0.3327
100	2.346	1.170	53.34	13.28	26.78	35.44	35.63	0.3343
120	2.336	1.162	52.88	13.07	26.74	34.92	35.45	0.3358
140	2.326	1.152	52.37	12.86	26.65	34.39	35.22	0.3373
160	2.315	1.143	51.83	12.64	26.55	33.84	34.98	0.3387